

Voltage-controlled Q switching of InGaAs/InP single quantum well lasers

K. Berthold, A. F. J. Levi, T. Tanbun-Ek, R. A. Logan, and S. N. G. Chu
AT&T Bell Laboratories, Murray Hill, New Jersey 07974

(Received 12 July 1989; accepted for publication 5 September 1989)

The light emission characteristics of high performance InGaAs/InP single quantum well laser diodes with a monolithically integrated intracavity loss modulator have been investigated. We demonstrate efficient voltage-controlled tuning of the lasing threshold current over more than one order of magnitude. In addition, active Q switching of 7 mW lasing light power with a change in electrical power of $< 30 \mu\text{W}$ is achieved.

Active Q switching of solid-state laser diodes is an efficient way to generate short optical pulses with high modulation depth and high repetition rates.^{1,2} Low switching power of active devices is attractive for high-speed optoelectronic signal processing.^{3,4} In addition, small capacitance and small switching voltages and currents are required for integration of lasers with low-power high-speed transistors.

In this letter we report for the first time active Q switching in buried-heterostructure graded-index separate-confinement heterostructure single quantum well (BH GRINSCH SQW) InGaAs/InP lasers utilizing a small area electroabsorption region. It is shown that the threshold current may be tuned over more than an order of magnitude by using a monolithically integrated intracavity loss modulator. We demonstrate that 7 mW lasing light power can be switched with a change in electrical power of $< 30 \mu\text{W}$.

InGaAsP crystals are grown by atmospheric pressure metalorganic vapor phase epitaxy (MOVPE). Epitaxial layers are grown on n^+ -InP substrates at 625 °C in a H_2 carrier gas using arsine, phosphine, trimethylgallium, and trimethylindium as sources. S and Zn, obtained using H_2S and dieth-

ylzinc, are the n and p dopants, respectively. Growth procedures for the GRINSCH SQW lasers do not utilize the insertion of InP spacer layers between the QW and the quaternary cladding layers as had been used previously to improve interface perfection in forming separate confinement quantum well lasers.⁵ Figure 1 shows a schematic diagram of the layer structure used. In the diagram, the band-gap wavelength λ_G of the quaternary compounds is indicated in micrometers and the thickness of the layers is given in nanometers. Figure 2 shows a cross-section transmission electron microscope image of a GRINSCH SQW structure with a quantum well thickness of $d = 5 \text{ nm}$. After removal from the growth chamber, buried-heterostructure lasers were formed using a procedure⁶ in which the wafers are stripe mesa etched, the width of the active region is reduced to $\sim 2 \mu\text{m}$ using a selective etch, and the samples are regrown with semi-insulating Fe-InP using MOVPE. Electrical contacts to the p^+ contact layer are achieved using three photolitho-

$\lambda_G = 1.0 \mu\text{m}$	InGaAsP	120 nm	$p = 2 \times 10^{16} \text{ cm}^{-3}$
	InP	1200 nm	$p = 2 \times 10^{17} \text{ cm}^{-3}$
	InP	50 nm	i
$1.0 \mu\text{m}$	InGaAsP	17 nm	i
$1.25 \mu\text{m}$	InGaAsP	20 nm	i
$1.33 \mu\text{m}$	InGaAsP	22 nm	i
$1.4 \mu\text{m}$	InGaAsP	23 nm	i
	InGaAs	d	i
$1.4 \mu\text{m}$	InGaAsP	23 nm	i
$1.33 \mu\text{m}$	InGaAsP	22 nm	i
$1.25 \mu\text{m}$	InGaAsP	20 nm	i
$1.0 \mu\text{m}$	InGaAsP	17 nm	i
	InP	1000 nm	$n = 1 \times 10^{18} \text{ cm}^{-3}$
	InP	SUBSTRATE	n^+

FIG. 1. Layer configuration of the InGaAs/InP GRINSCH SQW laser diodes with a quantum well thickness d . The InGaAsP band-gap wavelength λ_G is indicated in micrometers and the thickness of the layers is given in nanometers. Doping levels designated i are undoped, with background doping levels $\sim 10^{16} \text{ cm}^{-3}$ in InP and $\sim 10^{15} \text{ cm}^{-3}$ for InGaAs and InGaAsP.

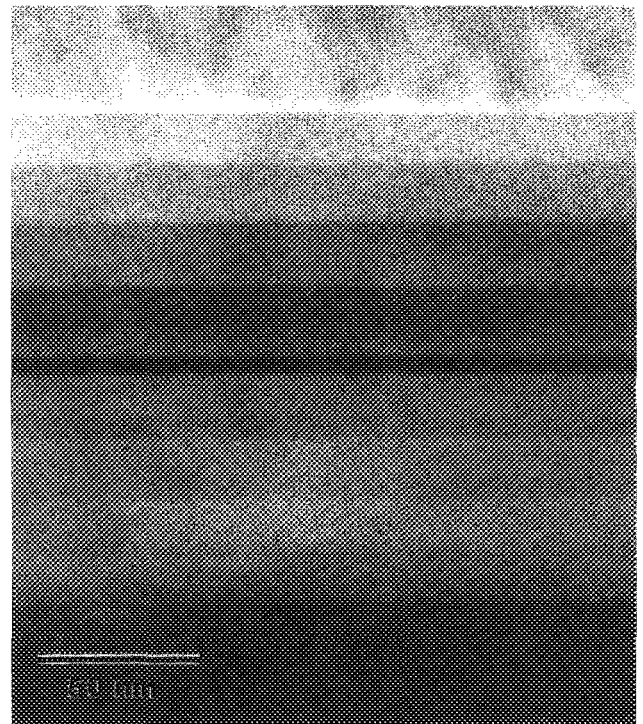


FIG. 2. Cross-section transmission electron microscope image of a GRINSCH SQW structure with an InGaAs quantum well of thickness $d = 5 \text{ nm}$.

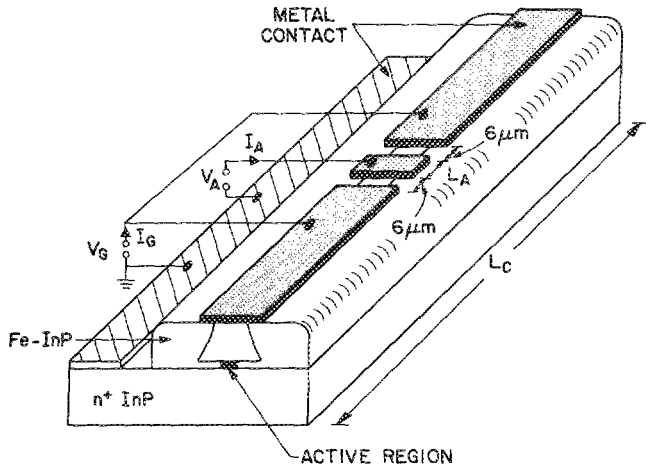


FIG. 3. Sketch of the BH GRINSCH SQW laser diode with a cavity length L_C and an absorber length L_A . The gain current I_G into the large segments, the absorber voltage V_A , and absorber current I_A at the small segment are indicated.

graphically defined metal stripes as shown in Fig. 3. The gap between the metal stripes is $6\ \mu\text{m}$ and the length of the small segment is $L_A = 6\ \mu\text{m}$. After etching off the p^+ -InGaAsP contact layer in the gap region, the resulting isolation resistance between the segments is $> 3\ \text{k}\Omega$. As illustrated in Fig. 3, the two long metal stripes are electrically connected and defined as the gain region, whereas the small section is defined as the modulator absorber region.

The single facet pulsed current light characteristic of a typical BH GRINSCH SQW laser diode with a quantum well thickness $d = 16\ \text{nm}$ and a cavity length $L_C = 300\ \mu\text{m}$

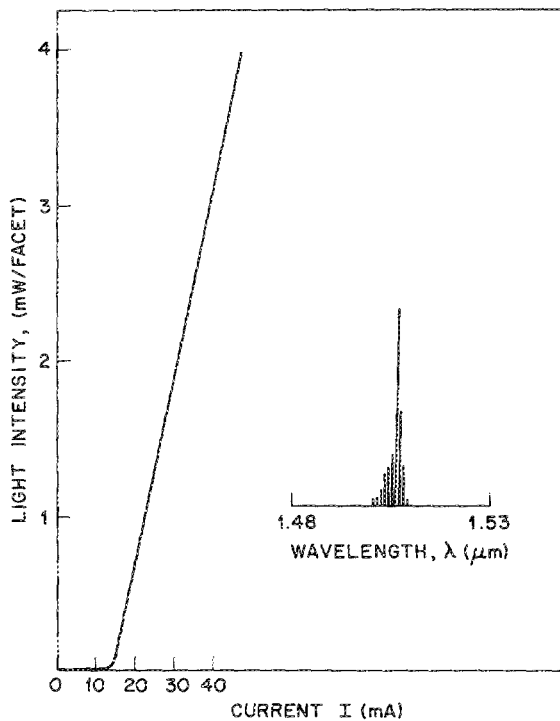


FIG. 4. Pulsed current light characteristic of a GRINSCH SQW laser diode with a cavity length $L_C = 300\ \mu\text{m}$ and with electrically connected small and large segments ($V_A = V_G$). The inset shows the light emission spectrum at a current $I = 40\ \text{mA}$.

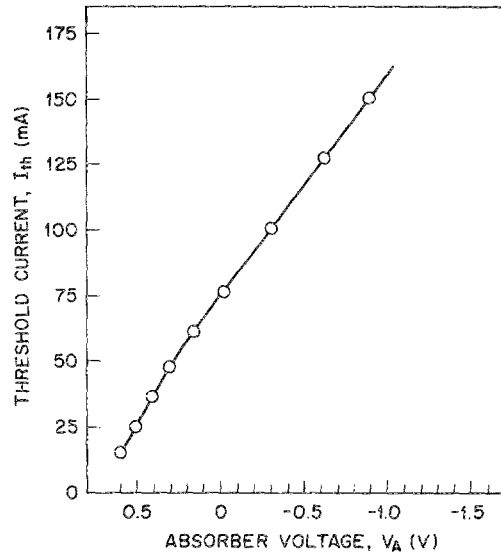


FIG. 5. Threshold current I_{th} vs absorber voltage V_A for a device of cavity length $L_C = 300\ \mu\text{m}$ and an absorber length $L_A = 6\ \mu\text{m}$.

is shown in Fig. 4. A threshold current of $I_{th} = 15\ \text{mA}$ is measured when the gain and absorber regions are electrically connected. To our knowledge, this is the lowest reported threshold current of any InGaAs/InP SQW laser.^{5,7} As may be seen from the inset of Fig. 4, the maximum emission of the laser is measured at a wavelength $\lambda = 1.51\ \mu\text{m}$. Results of photocurrent measurements and calculations of subband energies indicate that this wavelength corresponds to the transition between the heavy hole and the second quantized state in the conduction band. We note that lasing from the second subband has also been observed recently in GaAs SQW lasers and arises due to the higher available gain in the second subband.⁸⁻¹⁰

The dependence of threshold current I_{th} on absorber bias voltage V_A is illustrated in Fig. 5. As may be seen, the threshold current is tunable from $I_{th} = 15\ \text{mA}$ at a forward bias voltage $V_A = +0.6\ \text{V}$ to $I_{th} = 160\ \text{mA}$ at a reverse bias voltage $V_A = -1\ \text{V}$. This plot demonstrates strong modulation of threshold current with voltage applied to the small area intracavity absorber.

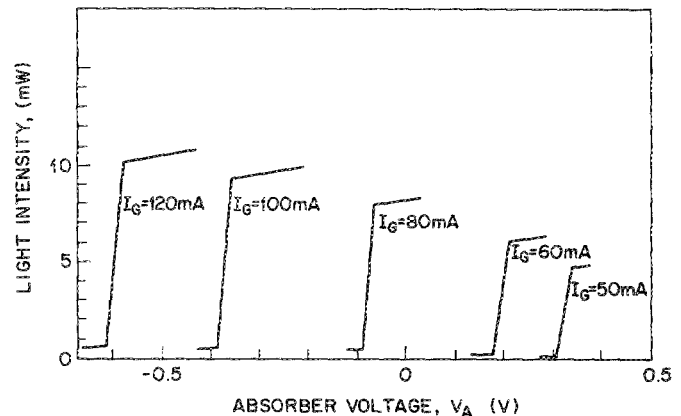


FIG. 6. Light intensity vs absorber voltage V_A for various gain currents I_G .

The total light output versus absorber bias voltage V_A is shown in Fig. 6 for various gain currents I_G . For a given gain current I_G 80 mA and for $V_A \approx 0$ V, the light intensity drastically changes from 8 to ~ 0.5 mW within a 30 mV change in absorber voltage. The photocurrent induced into the absorber region also decreases dramatically from 1.1 mA in the lasing state to 0.3 mA in the off state. With decreasing gain current the photocurrent decreases still further due to the lower lasing light power. These data demonstrate that at an operation voltage $V_A \approx 0$ V, 7 mW lasing light power may be switched with $< 30 \mu\text{W}$ change in electrical power.

The voltage-controlled operation of these three-terminal laser diodes is explained by electroabsorption involving the heavy hole state in the quantum well and the second quantized energy level in the conduction band.¹¹ The subband energy levels and the efficient tunability of absorption with bias voltage in these GRINSCH SQW structures are also supported by photocurrent measurements. With increasing reverse bias the measured photocurrent shows a strong increase at a wavelength $\lambda = 1.51 \mu\text{m}$, demonstrating efficient electrical tunability of the absorber.

In summary, we have demonstrated for the first time voltage-controlled operation of InGaAs/InP BH GRINSCH SQW laser structures. The threshold current may be tuned over more than one order of magnitude using a

small, low capacitance, monolithically integrated intracavity absorber. The observed tunability is due to electroabsorption involving the heavy hole and the second electron subband in the device. The efficient modulation capability of our structure is illustrated by switching 7 mW lasing light with $< 30 \mu\text{W}$ change in electrical power.

¹D. Z. Tsang, J. N. Walpole, Z. L. Liao, S. H. Groves, and V. Diadiuk, *Appl. Phys. Lett.* **45**, 204 (1984).

²Y. Arakawa, A. Larson, J. Paslaski, and A. Yariv, *Appl. Phys. Lett.* **48**, 561 (1986).

³D. A. B. Miller, *Opt. Lett.* **14**, 146 (1989).

⁴H. Liu, Y. Hashimoto, and T. Kamiya, *IEEE J. Quantum Electron.* **QE-20**, 43 (1989).

⁵T. Tanbun-Ek, H. Temkin, S. N. G. Chu, and R. A. Logan, *Appl. Phys. Lett.* **55**, 819 (1989).

⁶T. Tanbun-Ek, R. A. Logan, and J. P. Van der Ziel, *Electron. Lett.* **24**, 1483 (1988).

⁷Y. Miyamoto, M. Cao, K. Furuya, and Y. Suematsu, *Jpn. J. Appl. Phys.* **26**, L176 (1987).

⁸M. Mittelstein, Y. Arakawa, A. Larsson, and A. Yariv, *Appl. Phys. Lett.* **49**, 1689 (1986).

⁹Y. Tokuda, Y. Abe, T. Matsui, N. Tsukada, and T. Nakayama, *Appl. Phys. Lett.* **51**, 1664 (1987); Y. Tokuda, N. Tsukada, K. Fujiwara, K. Hamanaka, and T. Nakayama, *ibid.* **49**, 1629 (1986).

¹⁰K. Berthold, A. F. J. Levi, S. J. Pearton, R. J. Malik, W. Y. Jan, and J. E. Cunningham, *Appl. Phys. Lett.* **55**, 1382 (1989).

¹¹S. Schmitt-Rink, D. S. Chemla, and D. A. B. Miller, *Adv. Phys.* **38**, 89 (1989).